Forestry: An International Journal of Forest Research, 2025, 1–14
https://doi.org/10.1093/forestry/cpaf058
Original Article

Assessing the impacts of forest stand structure and landscape on the formation of *Ips typographus* damage hotspots in Finland

John Alexander Pulgarín Díaz [1,*], Juliana Pérez-Pérez[2], Markus Melin[3], Heli Peltola[1], Olli-Pekka Tikkanen[1]

[1]School of Forest Sciences, University of Eastern Finland, Joensuu, Finland, Yliopistokatu 7, Borealis, building A, Joensuu, Finland
[2]Department of Environmental and Biological Sciences, University of Eastern Finland, Yliopistokatu 7, Natura building, Joensuu, Finland
[3]Natural Resources Institute Finland (Luke), Yliopistokatu 6b, 80100 Joensuu, Finland
*Corresponding author. E-mail: alexander.pulgarin.diaz@uef.fi

Abstract

Damage caused by the European spruce bark beetle (SBB; *Ips typographus*) to Norway spruce (*Picea abies*) is expected to increase under climate change, particularly in Finland where Norway spruce is one of the most ecologically and economically important tree species. SBB damage often occurs in spatial hotspots (locations where high numbers of SBB damage cluster), with similar damage patterns in nearby locations. Evidence-informed decision-making requires an understanding of how stand and landscape attributes contribute to the formation of SBB damage hotspots. In this study, we analysed the impacts of stand and landscape attributes on SBB damage hotspots in the southern half of Finland, comprising 11.4 M ha of forestry land. We used data on SBB damage based on the spatial distribution of salvage logging operations due to SBB damage (a proxy for SBB damage) during 2012–20. The spatial autocorrelation of SBB damage was assessed using the global Moran's *I*, and we identified hotspots using local Moran's *I*. According to these, we classified the SBB-damaged stands as not forming hotspots, forming hotspots, or forming recurrent hotspots. Generalized linear mixed-effect models were used to examine how stand and landscape attributes influenced the probability of an infested area turning into a hotspot and the probability of a hotspot turning into a recurrent hotspot. Overall, SBB-damaged stands presented a low global spatial autocorrelation but still formed hotspots. Hotspots first aggregated in southeastern Finland, and thereafter also in the southwest. The low recurrence of hotspots over time suggests that the conditions necessary for sustained aggregation were not consistently met. While hotspot formation was associated with stand age and proximity to SBB damage during the previous two years, recurrent hotspots were more linked to stand development class and past damage proximity. The timely identification and removal of SBB-infested trees are crucial to reduce damage hotspot formation.

Keywords: areal data; Moran's *I*; local indicator of spatial association (LISA); point process analysis; evidence-informed decision-making

Introduction

The damage caused by the European spruce bark beetle, *Ips typographus* L. (SBB; Coleoptera: Curculionidae) to predominantly Norway spruce (*Picea abies* [L.] H. Karst.) forests in Europe is expected to increase in the coming years due to climate change (Hof and Svahlin 2016, Hlásny et al. 2021). The occurrence and degree of SBB damage are affected by different factors such as thermal conditions (Annila 1969, Wermelinger 2004), SBB population dynamics (Wermelinger 2004, Kautz et al. 2011), forest attributes (Wermelinger 2004, Kärvemo et al. 2014a), occurrence of storm damage (Eriksson et al. 2007), and landscape structure (Eriksson et al. 2007, Dobor et al. 2019). SBB damage tends to aggregate in specific locations where suitable conditions have aligned (Fig. 1), creating 'hotspots' where high levels of damage occur repeatedly over time (Stereńczak et al. 2020, Kamińska 2022).

SBB damage often occurs in clusters, with similar damage patterns in nearby locations (Stereńczak et al. 2020, Kamińska 2022). This aggregation is typical during epidemics, during which the beetles preferentially infest new hosts over short distances <500 m (Kautz et al. 2011, Kärvemo et al. 2014b), regardless of site conditions—e.g. nutrient-poor or low water retention soils (Christiansen and Bakke 1988, Netherer et al. 2019)—or host conditions—e.g. size, age, or health status (Wermelinger 2004, Hlásny et al. 2021)—leading to reports where all host individuals in one location are attacked (Stereńczak et al. 2020, Hlásny et al. 2021, Kamińska 2022). In addition, SBB and other bark beetles causing epidemics exhibit an aggregation behaviour, which contributes to the development of large-scale damage, as for example observed for *Dendroctonus ponderosae* Hopkins (Coleoptera: Curculionidae; (Nelson and Boots 2008, Bone et al. 2013). However, the contribution of stand- and landscape-level factors to the formation of SBB hotspots has not yet been studied in large spatially continuous regions at a regional or national scale. A large dataset comprising an extensive area and representing a wide range of ecological conditions allows us to examine how the formation of SBB hotspots varies across space and time, and to detect recurrence at the stand level—which is the smallest forest management unit in most Nordic countries.

Handling editor: Dr Fabian Fassnacht
Received 1 November 2024; **revised** 18 August 2025; **accepted** 23 August 2025

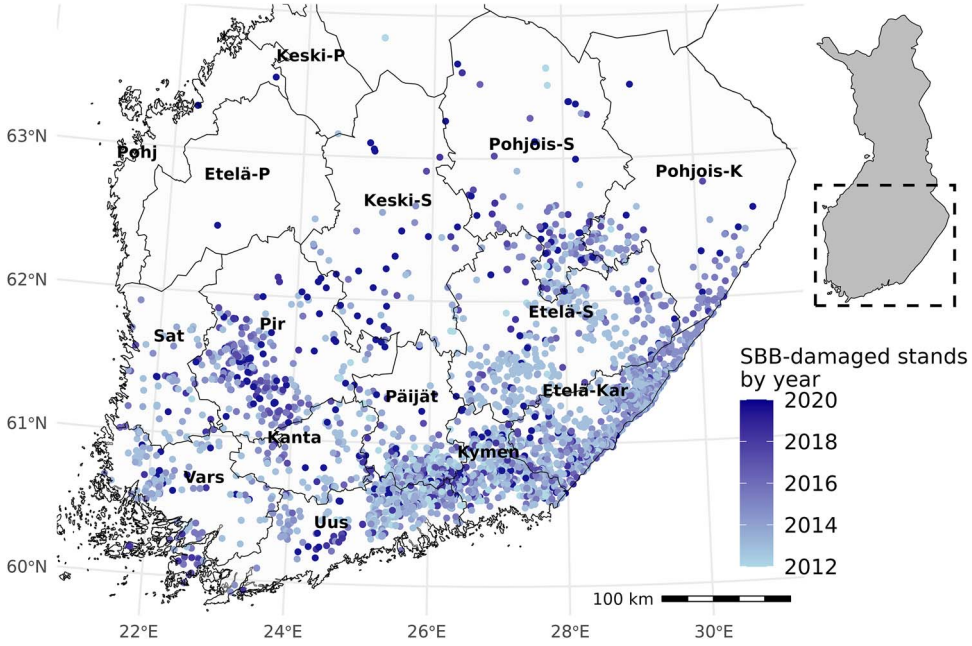

Figure 1. Reported salvage logged stands due to *I. typographus* (SBB) damage in the southern half of Finland (<64°N) 2012–20. Provinces: Etelä-Karjala (Etelä-Kar), Etelä-Savo (Etelä-S), Kainuu (Kainuu), Kanta-Häme (Kanta), Keski-Pohjanmaa (Keski-P), Keski-Suomi (Keski-S), Kymenlaakso (Kymen), Lappi (Lappi), Päijät-Häme (Päijät), Pirkanmaa (Pir), Pohjanmaa (Pohj), Pohjois-Karjala (Pohjois-K), Pohjois-Pohjanmaa (Pohjois-P), Pohjois-Savo (Pohjois-S), Satakunta (Sat), Uusimaa (Uus), and Varsinais-Suomi (Vars).

The aggregation of SBB damage has been documented in Poland (Stereńczak et al. 2019, Kamińska 2022) and Germany (Lausch et al. 2013) in studies focusing on smaller study areas. This phenomenon is not unique to this species; it is common across several bark beetle species and outbreak systems (Nelson and Boots 2008, Potter et al. 2016). In the case of SBB, damage aggregation has been frequently linked to predisposing disturbance events such as windthrows, which create favourable conditions for beetle establishment and spread (Økland et al. 2016).

To better understand the processes behind the formation of hotspots, spatial information in the form of damage report counts or rates (number of incident reports divided by the size of the at-risk population) is needed. Corresponding studies often use spatial autocorrelation (SA) as an indicator of the spatial relationship between damaged areas (Nelson and Boots 2008, Getis 2010). When SA is present, the samples may not be genuinely random, prompting the rejection of the sample independence assumption and thus requiring specialized techniques for analysis (Morales and López 2009, Siabato and Guzmán-Manrique 2019). For example, small-scale aggregated SBB damage has been found in Poland using both report counts and rates (Kamińska 2022).

The spatial formation and temporal recurrence of SBB damage and hotspots over large areas still remain poorly understood. Investigating these patterns is challenging, as it requires spatially explicit time-series data and substantial computational resources, which are often lacking (Anselin 1995). Yet, such research would allow not only to identify areas prone to damage (i.e. high-risk areas) but also to understand the factors driving emergence and recurrence of hotspots at the regional or national level. This can help improve early-warning systems by identifying patterns that precede hotspot formation. It also enables more targeted and cost-effective forest protection by helping managers prioritize monitoring and control efforts. Moreover, these findings can inform scenario analysis under alternative management or disturbance regimes, strengthening long-term strategic management planning (Venäläinen et al. 2020). Finally, spatially explicit outputs, such as maps indicating hotspot distribution could help in conveying the risks more efficiently to decision-makers and the broader public (Potter et al. 2016, Tobin et al. 2023).

In Finland, a better understanding of the impacts of different stand and landscape attributes on the occurrence of SBB damage hotspots is urgently needed for evidence-informed decision-making in forestry. To address this knowledge gap, we analysed the spatial distribution of salvage logging due to SBB damage from 2012 to 2020, as a proxy for SBB damage. Specifically, we (i) assessed the global SA of SBB damage at the landscape scale; (ii) identified locations where high numbers of SBB damage reports clustered into statistically significant hotspots; (iii) classified SBB-damaged stands based on hotspot formation (i.e. not forming hotspots [NoHH], forming hotspots [HH], or recurrent hotspots [RHH]); and (iv) explored how stand and landscape attributes influence the probability of an infested area turning into a hotspot and the probability of a hotspot turning into a recurrent hotspot. We hypothesized that SBB damage forms spatial hotspots that recur over time and that their patterns follow spatio-temporal patterns driven by stand attributes, prior damage, and forest management (e.g. salvage logging and distribution of clear-cuts). The identification of these patterns can support evidence-informed risk management related to SBB damage at the regional and national levels.

Methods

Study area and datasets

The study area encompassed the southern half of Finland, where most SBB damage currently occurs in the country (up to 64°N; Fig. 1). It includes a total of 11.4 M ha of mostly privately-owned forestry land available for wood production but excludes 0.383 M ha of protected areas, mostly state-owned (Korhonen et al. 2021). The region primarily consists of southern and middle boreal vegetation, with hemiboreal forests in the southwest and

middle boreal forests in the upland watersheds of central Finland (Korhonen et al. 2021). The study area is mainly lowlands but gradually increases in elevation to 200 m above sea level in a north-easterly direction (Nygren 2011). The forest is dominated by Scots pine (*Pinus sylvestris* L.) and Norway spruce (~33% of the total growing stock; Korhonen et al. 2021). Over the current climate reference period (1991–2020), the mean annual temperature varied from 6°C in the southern part of the study area (Helsinki, latitude 60.2°N) to 2.6°C in the north (Kajaani, latitude 64.2°N). Annual total precipitation varied from 680 mm in the south to 585 mm in the north (Finnish Meteorological Institute 2022).

To assess the spatial dynamics of SBB damage in Finland, we used spatial data from forest-use notifications that reported salvage logging due to SBB damage across the Finnish provinces (Fig. 1). Suomen Metsäkeskus (Finnish Forest Centre), the governmental authority for forestry administration in Finland, collects nationwide forest-use data from privately owned forests. Private forest owners are required by law to inform the centre of the reason for logging, which ensures the spatial continuity of the dataset. This dataset does not include state-owned forestry land, but the latter only accounts for 7% of the study area (Korhonen et al. 2021), so we consider its exclusion not to be a major concern.

We downloaded forest-use notifications filed between 2012 and 2020 on 18 October 2021, excluding duplicated reports. We focused on stands where Norway spruce was the main tree species (i.e. having the highest stocking volume), and where SBB damage or 'insect damage' was reported, leading to salvage logging. We included records of insect damage because SBB records were registered this way in the early years of salvage logging data collection. Moreover, only a few records exist where insects other than SBB (e.g. *Pityogenes chalcographus* L. [Coleoptera: Curculionidae]), caused enough damage to necessitate salvage logging.

The forest-use notifications dataset includes information on SBB-damaged stands and their attributes—including mean diameter at breast height (Dmean), mean stand age, site fertility class, and development class—obtained through remote sensing and field assessments (Metsäkeskus 2025). The average stand area in this dataset is 1.4 ha (Metsäkeskus 2021). The damage information is aggregated at the stand level, so neither the salvage logging volume nor a count of damaged trees is available in the dataset. Instead, we accounted for the intensity of logging events by aggregating the number of damaged stands to cells (see the Data Analysis section). More information on the stands having SBB damage can be found in our previous paper (Pulgarín et al. 2024).

Because the dataset lacks explicit information on the exact timing of the damage event, we followed Netherer et al. (2019) and Müller et al. (2022) to determine the most probable year of occurrence. For salvage logging operations between June and December, we assigned the damage to that same year. Conversely, for those from January to May, we attributed the damage to the previous calendar year, as prior studies suggest that any damage reported during this period likely originated in the previous year.

Data analysis

To study the spatial patterns of SBB damage at the landscape level, we created two rectangular grids covering the study area with cell sizes of 500 × 500 m and 1000 × 1000 m, respectively, with each cell representing one spatial unit (Fig. 2). Past research aggregating SBB damage data has used 1000 × 1000 m grids (Kamińska 2022) and 500 m diameter hexagons (Washaya et al. 2024), while prior research on *Dendroctonus ponderosae* has used 54 km^2 hexagons (Potter et al. 2016a). Setting a grid helps to ensure that most cells have neighbours, which is recommended for SA analysis (Bivand et al. 2008). It also maintains constant variation inside the cells while providing sufficient data for robust statistical analysis (Atkinson and Tate 2000). We used grids with 500 and 1000 m cell sizes corresponding to the maximum distance that SBB typically flies to attack new stands, making it meaningful for decision-makers. For example, a maximum dispersal distance of up to 750 m has been reported in Sweden (Müller et al. 2022, Kärvemo et al. 2014a).

We compiled SBB damage data (4579 observations) into the formed cells as their sums, based on the centroid of the salvage-logged polygon. A total of 4539 SBB damage reports were aggregated into the grids (i.e. their centroid fell inside a cell), while 40 observations fell outside the study area or the cell's centroid did not fall within any cell. In the 1000 m grid, 3058 cells contained SBB damage, compared to 3571 cells in the 500 m. Aggregating the number of damaged stands to the cell level helps to account for salvage logging intensity.

Assessing the spatial relationship between damaged areas

As an indicator of the spatial relationship between damaged areas, we assessed the SA between SBB-damaged stands in the study area, using the global Moran's index (Moran's I; $\alpha = 0.05$ (Moran 1950), which is a very common metric in SA studies (Banerjee et al. 2015, Siabato and Guzmán-Manrique 2019). It is equivalent to the measure of association in time series and is used to estimate the correlation function in point process studies (Banerjee et al. 2015). Moran's *I* assesses SA based on the locations of an object and its neighbours, indicating the degree of clustering for the population. Specifically, in our study, we assessed the extent to which cells with aggregated SBB-damaged stands are clustered with neighbouring cells with similar values or if they are randomly located. For the global Moran's *I* calculation, we used the number of damaged stands within each cell. Moran's *I* is centred on the mean, meaning that the model has a constant mean, and any SA is likely caused by the relationship between units, or the spatial weights given to the neighbours according to their relationship (Anselin 1995, Bivand et al. 2008). Moran's I ranges from −1 to 1, where values close to 1 indicate positive SA (i.e. cells with similar values are close together), values close to −1 indicate negative SA (i.e. cells with similar values are dispersed), and values close to 0 indicate a random dispersion of cell values (Siabato and Guzmán-Manrique 2019).

SA studies in human epidemiology often use rates (i.e. number of cases per at-risk population) to adjust for population size, particularly for infectious diseases where the at-risk population remains relatively constant (Siljander et al. 2022). While rates help account for population size, they can inflate risk in small populations and mask hotspots in large ones (Bivand et al. 2008, Darikwa and Manda 2022), misrepresenting outbreak severity and hindering mitigation efforts. Considering SBB outbreaks, the at-risk population decreases as trees die or are logged, making rates a less reliable approach. Therefore, we used counts, which is preferred when assessing risk. This is because each report represents a potential driver of new cases and better reflects outbreak dynamics (Salas et al. 2021, Perez-Perez et al. 2025).

After aggregating damage reports to the cells, we identified neighbouring cells using two methods. In the first method, referred to as the 'queen' method, all cells touching the assessed cell (including at the corners) were defined as neighbouring cells. In the 500 m grid, the closest cells were 250 m from the centroid of the assessed cell, while neighbouring corner cells were located

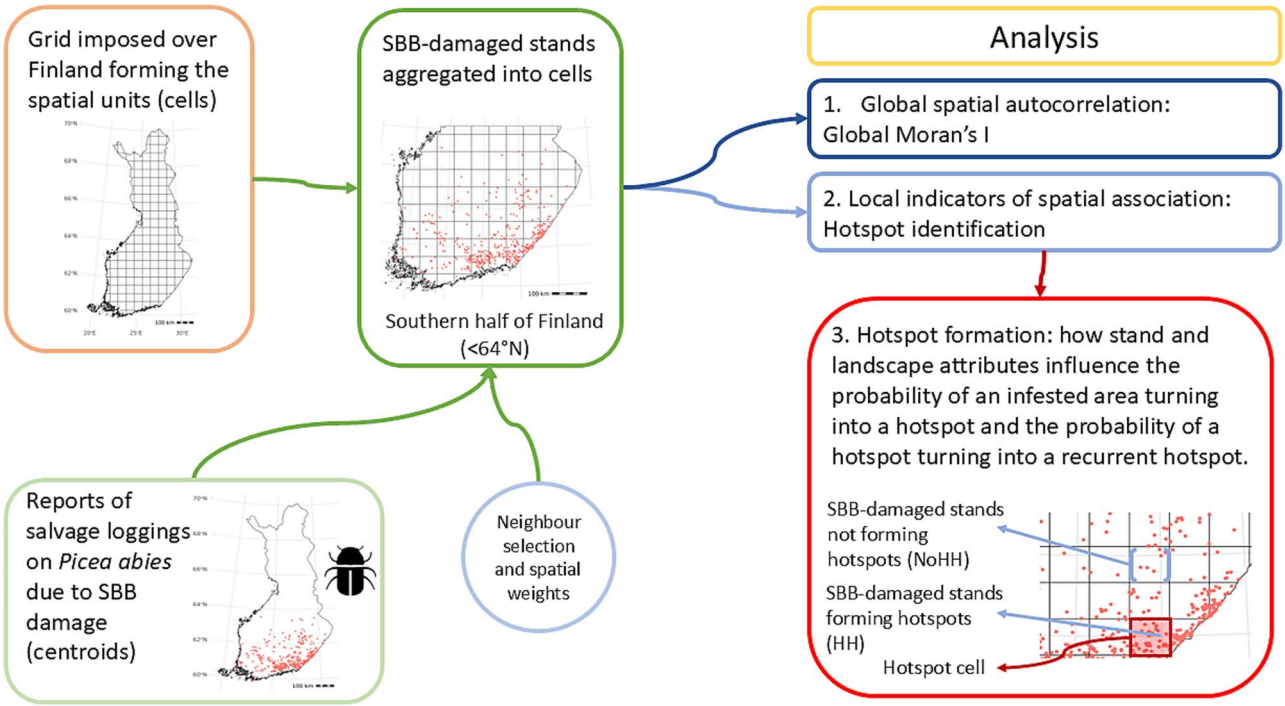

Figure 2. Methodology for assessing the spatial dynamics of salvage logging as a proxy for *I. typographus* (SBB) damage in Finland, 2012–20.

at a distance of 353 m. In the 1000 m grid, the closest cells were 500 m from the centroid and the neighbouring corner cells were at 707.1 m away, similar to previous studies of SBB SA (Kamińska 2022). The second method we used was a distance threshold from the cell border: in the 500 m grid, neighbourhoods were formed with cells whose centroids were within 500, 750, or 1000 m of the assessed cell. For the 1000 m grid, the neighbourhood consisted of cells whose centroids were within 1000, 1500, or 2000 m of the assessed cell. These values were chosen based on the distance where new SBB damage could be reasonably expected to occur according to the SBB dispersal abilities to attack new stands (Kärvemo et al. 2014a, Müller et al. 2022). In both methods, we followed previous research and discarded those cells without neighbours (Nardi et al. 2023).

We next assigned spatial weights to neighbours to indicate their spatial relationship. For this, we used the row-standardization style, which "gives a weight of unity to each neighbour relationship, then it divides these weights by the per unit sums of weights" (Pebesma and Bivand 2023). We then adjusted these weights to attenuate when the distance between the cells' centroids increased, to account for the decreasing probability of new SBB damage with greater distance from earlier damage (Kautz et al. 2011, Stereńczak et al. 2019, Müller et al. 2022). We calculated the global Moran's *I* and assessed its significance using a Monte Carlo simulation approach (9999 permutations; $P < .05$). The simulation randomly shuffled the observed values and calculated the Moran's *I* before determining the sampling distribution (Anselin 1995, Banerjee et al. 2015). Using these spatial weight settings, each method of neighbour selection (i.e. the queen method and the distance threshold) is weighted differently, meaning we cannot directly compare global Moran's *I* across the methods. To compare across neighbour-selection methods, we used z-values that correct the effect of the weights using the expected value of global Moran's *I* and its variance (O'Sullivan and Unwin 2010, Siabato and Guzmán-Manrique 2019).

Identification of hotspots

The global Moran's*I* reflects the SA trend for the whole study area, but to identify hotspots locally and understand which attributes affect them, we used the local Moran's *I*, also called the local indicator of spatial association (LISA; Anselin 1995). To calculate it, we used the 500 m grid and the queen neighbour-selection method, as it is more representative of the SBB dispersion (other neighbour-selection methods and the 1000 m grid yielded similar SA results, see the Spatial Relationship between Damaged Areas section). The parameters for the LISA analysis were the same as the global Moran's *I* (see the Spatial Relationship between Damaged Areas section). LISA yields four categories of spatial association for the studied phenomenon: 'High–High' cells where high values are surrounded by similar entities; 'Low–Low' cells where low values are surrounded by similar entities; 'High–Low' cells where high values are surrounded by entities with low values; and 'Low–High' cells where low values surrounded by entities with high values. We focused only on the High–High category, which represents cells with a high number of aggregated SBB-damaged stands surrounded by other high-value cells with similar values, referred to as 'hotspots' (Anselin 1995, Anselin 1996, Pebesma and Bivand 2023). This clustering of SBB damage highlights critical locations that require focused attention from forest managers.

To identify SBB damage hotspots and their temporal recurrence, we grouped the annual damage reports into three 3-year windows for the LISA analysis (i.e. 2012–14, 2015–17, and 2018–20). This approach, also used in previous bark beetle studies (e.g. Potter et al. 2016), reduces short-term noise, improving the stability and interpretability of spatial clusters (Anselin 1995, Pebesma and Bivand 2023). In addition, a 1-year timescale may obscure the delayed effects of earlier SBB damage and fail to capture the persistence of damage patterns as earlier shown in Germany (Lausch et al. 2013). This time-windows approach also helped to reduce the confounding influence of SBB damage older than 2 years on the formation of hotspots while still accounting for the effect of damage from the two previous years. Incorporating

these lagged effects led us to block the present year and the two previous years to identify hotspots. To reduce the risk of false positives in identifying hotspots—i.e. cells incorrectly classified as statistically significant hotspots when no real clustering exists—we used a stricter significance threshold of $P < .005$. Meaning that, there is only a 0.5% probability that a cell is incorrectly identified as a hotspot. Thus, even in the absence of true hotspots, ∼0.5% of the cells are expected to be identified as significant by chance. Additionally, we applied the false discovery rate correction proposed by Brunsdon and Comber (2015), further controlling for the expected proportion of false positives among the identified hotspots.

Analysis of the effects of forest and landscape attributes on hotspot formation

We next classified each SBB-damaged stand based on whether its centroid fell within a hotspot cell. Stands were categorized as: not forming hotspots (NoHH), forming hotspots (HH), or forming recurrent hotspots (RHH) if they appeared more than once during the study period (see Fig. 2 part 3 for a graphical illustration of this definition). This classification resulted in a new attribute assigned to each SBB-damaged stand: NoHH, HH, or RHH. We then used binary generalized linear mixed-effect models (GLMMs) with a logit link function, to examine how stand and landscape attributes influenced (first model) the probability of an infested area turning into a hotspot and (second model) the probability of a hotspot becoming a recurrent hotspot (see Fig. 2 part 3). Stand attributes included Dmean, stand age, site fertility class, and stand development class. Site fertility classes were 'herb-rich forest', 'herb-rich heath forest', 'mesic heath forest', and 'sub-xeric heath forest'. Stand development classes included 'shelter-tree stand', 'mature stand', 'advanced stage stand', and 'low-yielding forest' (Table S1).

Landscape attributes included the Euclidean distances from an SBB-damaged stand to the closest clear-cut and the closest SBB-damaged stand from the previous 2 years, using the stands' centroids. We identified clear-cuts using a nationwide geo-dataset, downloaded on 17 November 2021, which contains information about the structure of all privately owned Finnish forests (e.g. mean age, mean height, basal area, stem count, and volume). The data were collected through both remote sensing and fieldwork (Metsäkeskus 2025). As clear-cuts, we classified all stands <5 years old (regardless of the tree species), for each of the studied year (i.e. 2012–20), according to the last updated stand age. Using this dataset to identify clear-cuts helped us to confirm the final area of the selected clear-cuts and the year of the logging operation, as the notified and the actual operation might vary in terms of area and year. These clear-cuts can create favourable conditions for SBB reproduction, regardless of whether they originate from salvage logging or regular forestry practices. These conditions include the presence of weakened or wind-damaged trees (Louis et al. 2015, Hroššo et al. 2020) and increased edge temperatures, which accelerate beetle development, promote flight activity and dispersal, and intensify the synchrony and strength of mass attacks (Funke and Petershagen 1994, Wermelinger and Seifert 1999, Wermelinger 2004, Hinze and John 2019, Lindman et al. 2023). Together, these conditions improve the beetles' capacity to coordinate attacks and overcome host defences.

To fit the GLMMs, we considered the spatial and temporal grouping and unbalanced structure of the data by defining random effects for the Finnish 'province' where the damage occurred and the respective 'year', following Equation (1). These random effects (province and year) account for unobserved heterogeneity and correlation among observations (see Assessing the Spatial Relationship between Damaged Areas section) within provinces and years, thereby improving model fit. They also help capture intra-group correlation, absorb unexplained variation, and reduce bias in the estimation of fixed effects (Hilbe 2009).

$$\begin{aligned} y_{ij} &\sim Bernoulli\ (p_{ij}) \\ logit\,(p_{ij}) &= \mathbf{x}'_{ij}\boldsymbol{\beta} + a_i + b_j + \epsilon_{ij} \end{aligned} \tag{1}$$

In Equation (1) and in the first model, y_{ij} is a binary indicator taking 1 if the SBB-damaged stand turns into a stand forming a hotspot (HH) in province i in year$j$ and 0 otherwise. In the second model, y_{ij} equals 1 if the SBB-damaged stand turns into a stand forming a recurrent hotspot (RHH) in province i in year$j$ and 0 otherwise. p_{ij} is the probability of forming an HH or an RHH in the two studied models in province i **in year** j; $\mathbf{x}'_{ij}\boldsymbol{\beta}$ is the fixed predictor variables with the corresponding coefficient vector $\boldsymbol{\beta}$; a_i (for province) and b_j (for year) are the normally distributed random effects with a mean of zero and constant variances; and ϵ_{ij} is the vector of random errors. This model helps to measure the association between the stand and landscape attributes and the formation of HH and RHH ($\alpha = 0.05$; Diaz-Quijano 2016).

We found that the distribution of SBB-damaged stands has SA (Assessing the Spatial Relationship between Damaged Areas section), indicating that they interact and lack independence (Siabato and Guzmán-Manrique 2019), potentially leading to under- or overdispersed models (Morales and López 2009, Morales and Lozano 2014). Underdispersion occurs when the observed variance is lower than expected under the theoretical model, and overdispersion occurs when the observed variance exceeds that expected by the theoretical model (Morales and López 2009, Morales and Lozano 2014). This misspecification can lead to biased parameter significance, incorrect and overly complex models, and imprecise predictions (Morales and López 2009, Morales and Lozano 2014). In addition to the previously described model settings, we log-transformed the distance variables using 'log(1 + distance)' to account for zero values and improve model fit. In addition, we truncated the distance to earlier SBB-damaged stands at a threshold, assuming that the effect of earlier damage declines with distance (Kärvemo et al. 2014a, Müller et al. 2022). Beyond this threshold, the predictor's influence stops growing, avoiding overestimation at extreme distances, as in previous research (Rhodes et al. 2009). This approach also reduced overdispersion and improved the model performance. Since HH and RHH classifications were not present in all fertility and stand development classes, we focused on those classes where they appeared to avoid perfect separation, as well as problems in model convergence and in the calculation of standard errors. We checked collinearity between fixed effects (stand and landscape attributes) using the variance inflation factor. This factor helped to identify predictors that may inflate the variance of regression coefficients when two or more variables are collinear, making the model less stable and harder to interpret (Sikkink et al. 2007). If it exceeds 10, collinearity might be problematic, although some authors recommend conservative thresholds (Sikkink et al. 2007, Zuur et al. 2009). For our analysis, its value remained below 4, indicating no significant collinearity among the predictors (Table S2).

To check the models' goodness of fit, we used the dispersion statistic (Pearson X^2 statistic divided by the degrees of freedom of the residuals) to quantify dispersion (Hardin and Hilbe 2007,

Table 1. Spatial autocorrelation of *I. typographus* (SBB)-damaged stands (salvage logging) in Finland (2012–20) measured with global Moran's *I*, using varied grid sizes and different neighbour-selection methods.

Grid cell size	Neighbour-selection method	Moran's *I*	z-value	Pseudo-*P*
500 m	Queen[a]	0.106	87.597	<.001
	Same grid distance (500 m)	0.133	85.232	<.001
	1.5× grid distance (750 m)	0.111	88.344	<.001
	2× grid distance (1000 m)	0.098	89.307	<.001
1000 m	Queen	0.177	82.648	<.001
	Same grid distance (1000 m)	0.194	76.378	<.001
	1.5× grid distance (1500 m)	0.176	83.272	<.001
	2× grid distance (2000 m)	0.163	86.056	<0.001

[a]The 500 m grid with the queen neighbour selection method was used for LISA analysis, as they are more representative of the SBB-damage distribution process. For more details, see the Identification of Hotspots section.

Hilbe 2009, Mehtätalo and Lappi 2020), the sample variogram to test the SA of the residuals, and the Durbin–Watson test to assess the temporal autocorrelation. If the dispersion statistic is >1.0, overdispersion is likely. If it is <1.0, underdispersion is probable (Hilbe 2009). An increasing trend in the sample variogram suggests increasing spatial autocorrelation with decreasing distance (Pinheiro and Bates 2000). The Durbin–Watson test assesses the temporal autocorrelation of scaled residuals (Hartig 2024).

For all the processes we used RStudio v.2023.12.0 + 369 (RStudio Team 2023) with the following packages: Simple Features 'sf' version 1.0–5 (Pebesma 2018) for the geographical analysis; 'glmmTMB' version 1.1.7 (Brooks et al. 2017) for the modelling process; 'performance' version 0.12.4 (Lüdecke 2018) to calculate the variance inflection factor; 'ggpredict' version 1.7.2 (Lüdecke 2018) to generate model-based estimates for each statistically significant variable; 'DHARMa' version 0.4.7 (Hartig 2024) to evaluate the temporal autocorrelation; 'car' version 3.1-3 (Fox and Weisberg 2019) to calculate the analysis of deviance; and 'gstat' version 2.1-2 (Gräler et al. 2016) to calculate the sample variogram.

Results

Spatial relationship between damaged areas

The global SA was consistent across different grid and neighbour-selection methods, ranging from 0.098 to 0.194 (all statistically significant) with very similar SA strengths (i.e. z-values; Table 1). These results provide evidence for rejecting the null hypothesis of randomly distributed SBB damage across the space, as there is a significantly low-to-moderate SA and increasing strength as the distance between neighbours increased, independent of the grid size, reinforcing the robustness of the spatial signal.

Identified hotspots

We identified several locations of spatially clustered SBB damage, resulting in statistically significant hotspots (Fig. 3). Out of the 3571 cells with aggregated SBB damage reports, 1406 (39.4%) formed hotspots (Table 2). We found that the SBB-damaged stands appeared and disappeared over the three 3-year time windows (Fig. 3). Hotspots were primarily concentrated in the southeast, where they occurred throughout the study. However, there were very few hotspots in the last time window (2018–20). The identified hotspots diffused in a wave pattern, with the largest proportion of hotspots in the first time window in the southeastern part of the study area (Fig. 3 and Table 2).

Over time, the number of hotspots decreased, reaching the lowest number at the end of the study period (Table 2). While hotspots did occur in the western part of the study area, the numbers were relatively small. While the northern part of the study area had SBB damage events, very few hotspots formed, despite the presence of susceptible Norway spruce stands (Figs 1, 3, and 4). The discovered hotspots were not particularly recurrent, as only 3.7% of the hotspots from the first time window recurred in the second time window, and 3.8% of the hotspots from the first time window recurred in the last time window (Fig. 3 and Table 2). The discovered recurrent hotspots only occurred in the southeast of the study area (Fig. 4), with 26 in Etelä-Karjala (74.3%), six in Päijät-Häme (17.1%), two in Uusimaa (5.7%), and one in Etelä-Savo (2.8%).

Effects of forest and landscape attributes on hotspot formation

The assessment of the models' fit to the data showed no signs of significant under- or overdispersion (Dispersion statistic in Tables 3 and 4), or spatial autocorrelation (Fig. S1) or temporal autocorrelation (temporal autocorrelation [P-value = 0.156] in Tables 3 and 4). As a result, the models can reasonably be used to identify the attributes that increase the probability of an SBB-damaged stand becoming a hotspot and the probability of a hotspot becoming a recurrent hotspot. In the model assessing whether an SBB-damaged stand becomes a hotspot, most of the random variations were found at the year level; when assessing whether a hotspot became a recurring hotspot, the random variation was allocated at the province level.

A few of the studied attributes influenced the probability of an infested area becoming an HH (Tables 3 and 5) and that of an HH becoming an RHH (Tables 4 and 5). As expected, proximity to the SBB-damaged stands in the previous 2 years influenced HH and RHH formation (Figs 5 and 6). The probability of an SBB-damaged stand becoming an HH also increased with stand age, although with a lower strength. No significant differences were found when comparing to the reference level for fertility and development class. When evaluating the overall effect of fertility class and stand development class using an analysis of deviance (Wald chi-square tests), only the stand development class was statistically significant and for the recurrent hotspots model (Table 5). In both models, distance to SBB_{y-1} was the most influential attribute with a dramatic decrease in the probability when the distance was >500 m. SBB_{y-1} also had a greater influence on the HH and RHH formation than SBB_{y-2} (Tables 3 and 4). For the truncated distances, the probability did not change after the indicated threshold.

Discussion

We analysed how stand and landscape attributes influence the SBB damage hotspot formation in southern Finland using salvage

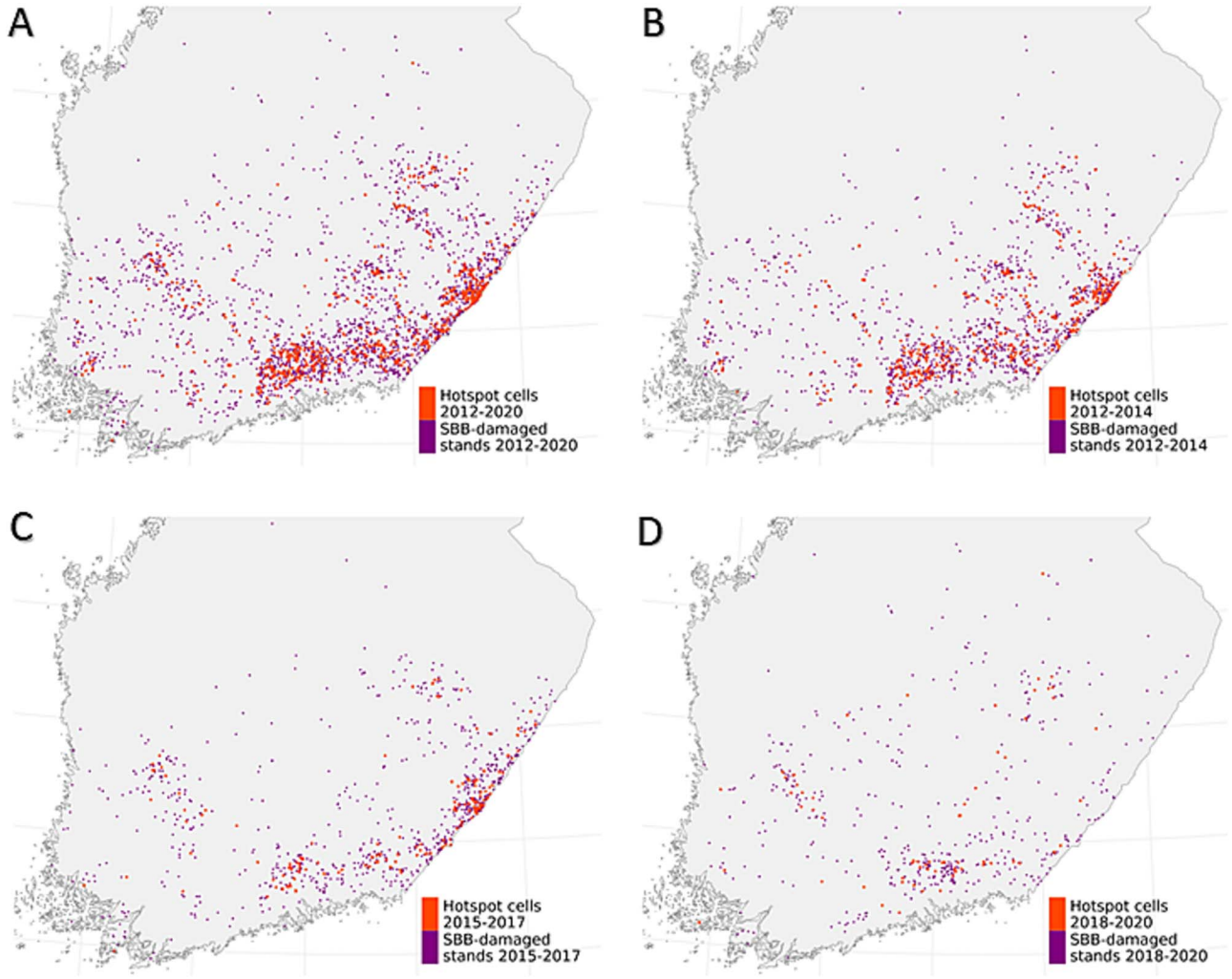

Figure 3. *Ips typographus* (SBB)-damaged stands forming hotspot cells (500 m) in Finland: (A) 2012–20 (entire study period); (B) 2012–14; (C) 2015–17; and (D) 2018–20.

Table 2. Number of *I. typographs* (SBB) damage reports aggregated into spatial units (500 m cells), forming hotspots and recurrent hotspots in Finland based on LISA analysis.

Time window	Number of SBB-damage reports	Number of hotspot cells	Number of recurring hotspot cells
2012–14	2624	907	N/A
2015–17	1236	352	34
2018–20	679	147	35

logging data from 2012 to 2020. We studied the spatial relationship between damaged areas by calculating the SA of SBB damage using the global Moran's *I*. We identified SBB hotspots using the local Moran's *I* and classified SBB-damaged stands according to their formation of hotspots. Global SA was low to moderate, but hotspots formed locally—initially in the southeast, later also in the southwest. Hotspot formation correlated with stand age and proximity to SBB-damaged stands in the previous 2 years. Recurrent hotspot formation correlated with stand development class and proximity to older damage. Our study may help elucidate the drivers of SBB-damage dispersion, hotspot, and recurrent hotspot formation, providing support for evidence-based decision-making regarding SBB-damage risk management at the regional and national levels.

The spatial relationship between damaged areas

To the best of our knowledge, the spatial distribution of SBB damage in Finland has not previously been studied to this extent. We found a low global SA, even after using different grids and neighbour-identification methods, indicating a spatial link between SBB damage at a large scale. Moreover, the increasing SA strength with broader neighbour definitions suggests that spatial clustering is consistent over larger spatial scales. Altogether, this point to a spatially dependent process driving SBB damage distribution, likely influenced by factors operating beyond the stand scale and into the surrounding landscape.

While the low global SA found in our study contradicts past research showing a high SA for SBB damage, that past research was conducted at the tree scale in smaller study areas. These

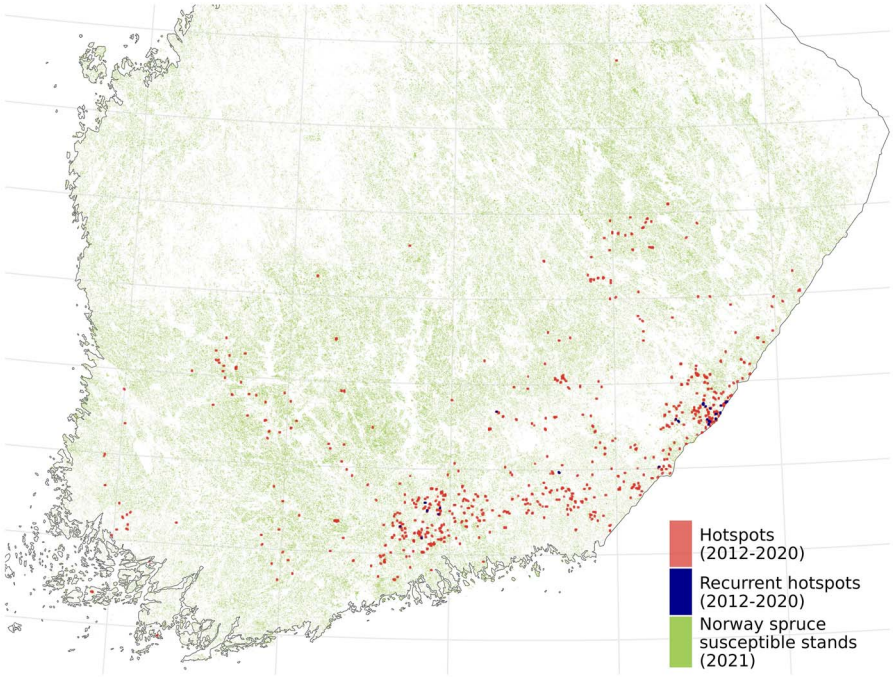

Figure 4. Susceptible *Picea abies* stands (green) defined as stands where *P. abies* is the main tree species, with a stand mean diameter > 15 cm and a stand mean age > 25 years—extracted from a nationwide geo-dataset that contains information about the structure of all privately owned Finnish forests (Metsäkeskus 2025, Pulgarín et al. 2024). Also shown are hotspots (orange) and recurrent hotspots (blue) of *I. typographus* damage in Finland, identified using LISA analysis on 500 m cells.

Table 3. Summary of the generalized linear mixed-effects model showing the effects of attributes on the probability of an *I. typographus*-damaged stand turning into a stand becoming a hotspot.

Fixed effects	**Estimate**	**Std. error**	**z-value**	**Pr(>|z|)**
Intercept	3.691	1.470	2.511	0.012
Stand mean diameter at breast height	−0.020	0.019	−1.068	0.285
Stand mean age	0.012	0.003	3.189	0.001
Development class: advanced stage stand[a]	−0.162	0.598	−0.271	0.786
Development class: mature stand	−0.270	0.583	−0.464	0.642
Development class low-yielding forest	−0.373	0.611	−0.610	0.541
Fertility class: herb-rich heath forest[a]	1.885	1.080	1.746	0.080
Fertility class: mesic heath forest	1.945	1.079	1.802	0.071
Fertility class: sub-xeric heath forest	1.858	1.154	1.610	0.107
log(1 + distance to clear-cut)	0.007	0.036	0.198	0.843
log(1 + distance to SBB_{y-1})	−0.621	0.051	−12.158	<0.001
log(1 + distance to SBB_{y-2}, truncated to 1 km)	−0.183	0.087	−2.092	0.036
Random effects		Variance	Std.Dev.	Groups
Province	Intercept	4.74E-09	6.89E-05	15
Year	Intercept	0.023	0.152	7
Model evaluation				
Dispersion statistic	1.081			
Temporal autocorrelation (Durbin–Watson)	1.749	*P*-value	0.723	
Number of observations	1721			

[a]The reference classes were 'shelter-tree stand' for the development class and 'herb-rich forest' for the fertility class. $SBB_{(y-1 \text{ or } y-2)}$ = closest SBB-damaged stand in the previous 2 years.

found, e.g. Moran's *I* of 0.48–0.54 in one study (Stereńczak et al. 2019) and 0.39–0.58 in another (Kamińska 2022). Our study data did not support such a detailed analysis as the damage information was aggregated at the stand level. Other explanations for the low global SA in our study may be that: (i) the real association for our phenomenon is not linear between neighbours (Anselin 1995) or (ii) that some SBB-damaged stands may have gone unreported, been misidentified, or were not salvage-logged. Large variation in SA regimes is also common in large spatial datasets (Anselin 1995, Anselin 1996). It is also important to note that Finland is situated on the northern perimeter of the SBB distribution. The temperature in this region constrains reproduction (Wermelinger 2004) and prevents SBB damage from spreading as widely as in Central European countries (Hlásny et al. 2021), where high SA has

Table 4. Summary of the generalized linear mixed-effects model showing effects of attributes on the probability of an *I. typographus* (SBB)-damaged stand forming a hotspot becoming a stand forming a recurrent hotspot.

Fixed effects	**Estimate**	**Std. error**	**z-value**	**Pr(>|z|)**
Intercept	6.089	4.120	1.478	0.139
Stand mean diameter at breast height	−0.037	0.069	−0.539	0.589
log(stand mean age)	0.122	1.088	0.112	0.910
Development class: advanced stage stand[a]	−1.314	1.136	−1.156	0.247
Development class: mature stand	−1.097	1.004	−1.093	0.274
Development class: low-yielding forest	0.258	1.078	0.24	0.810
Fertility class: mesic heath forest[a]	−0.244	0.405	−0.603	0.546
log(1 + distance to clear-cut)	−0.091	0.110	−0.831	0.405
log(1 + distance to SBB_{y-1}, truncated to 4 km)	−0.644	0.169	−3.809	<0.001
log(1 + distance to SBB_{y-2}, truncated to 4 km)	−0.378	0.123	−3.052	0.002
Random effects		Variance	Std.Dev.	Groups
Province	Intercept	0.575	0.7579	10
Year	Intercept	1.30E-08	0.0001	5
Model evaluation				
Dispersion statistic	1.009			
Temporal autocorrelation (Durbin–Watson)	0.958	*P*-value	0.156	
Number of observations	494			

[a]The reference classes were 'shelter-tree stand' for the development class and 'herb-rich heath forest' for the fertility class. $SBB_{(y-1 \text{ or } y-2)}$ = closest SBB-damaged stand in the previous 2 years.

Table 5. Analysis of deviance (Type II Wald chi-square tests) for the generalized linear mixed-effects models showing the effects of attributes on the probability of an *I. typographus*-damaged stand becoming a stand forming a hotspot, and such hotspots becoming a stand forming a recurrent hotspot.

Hotspots	**Chisq**	**d.f.**	**Pr(>Chisq)**
Stand mean diameter at breast height	1.141	1	0.285
Stand mean age	10.16	1	0.001
Stand development class	1.045	3	0.790
Site fertility class	3.461	3	0.325
log(1 + distance to clear-cut)	0.039	1	0.843
log(1 + distance to SBB_{y-1})	147.806	1	<0.001
log(1 + distance to SBB_{y-2}, truncated to 1 km)	4.3785	1	0.036
Recurrent hotspots			
Stand mean diameter at breast height	0.2909	1	0.589
log(stand mean age)	0.0126	1	0.910
Stand development class	10.5727	3	0.014
Site fertility class	0.3639	1	0.546
log(1 + distance to clear-cut)	0.6911	1	0.405
log(1 + distance to SBB_{y-1}, truncated to 4 km)	14.5116	1	<0.001
log(1 + distance to SBB_{y-2}, truncated to 4 km)	9.3129	1	0.002

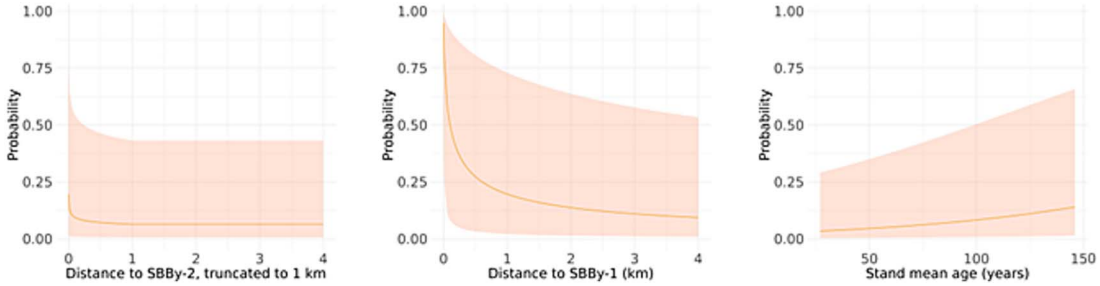

Figure 5. Probability of an *I. typographus* (SBB)-damaged stand forming a hotspot based on the fixed effects for the statistically significant attributes. Other variables are held constant at their mean (for continuous variables) or at the reference level (for categorical variables). $SBB_{(y-1 \text{ or } y-2)}$ = nearest SBB-damaged stand in the previous 2 years. The shaded area represents the 95% confidence interval.

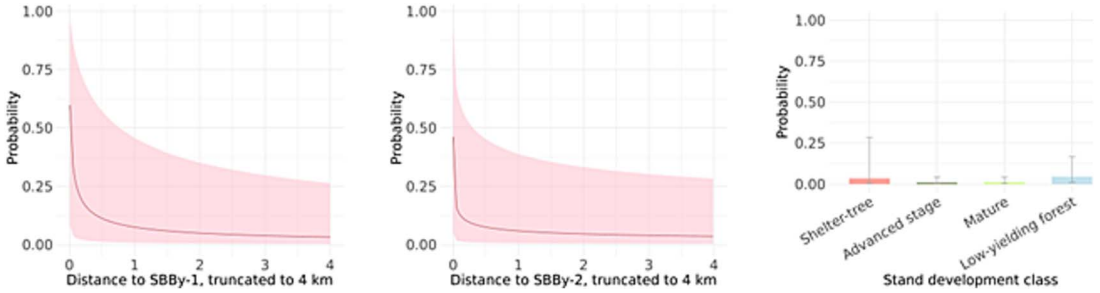

Figure 6. Probability of an *I. typographus* (SBB)-damaged stand forming a hotspot to become a recurrent hotspot based on the fixed effects for each statistically significant attribute. Other variables are held constant at their mean (for continuous variables) or at the reference level (for categorical variables). $SBB_{(y\text{-}1 \text{ or } y\text{-}2)}$ = nearest SBB-damaged stand in the previous 2 years. The shaded area represents the 95% confidence interval.

been reported (Stereńczak et al. 2019, Kamińska 2022). Our LISA analysis, however, revealed areas where SBB damage aggregated into hotspots. Based on the observed distribution of reported salvage logging operations, we propose that the distribution patterns and hotspots associated with SBB damage closely mirror those of other species, for which occurrence and abundance decline towards the edge of the range (Brown et al. 1995, Sexton et al. 2009).

Research on SBB distribution and SA covering extensive regions and extended time periods has so far been largely lacking in Finland. Our study covered 9 years of SBB damage data at a nationwide scale, but the SBB damage was limited to the southern half of Finland. Studies of this kind are constrained by the availability of spatially explicit data and analytical challenges, including neighbour selection and the definition of spatial weights—issues we addressed in this study.

Formation of hotspots and recurrent hotspots and factors contributing to them

It is expected that SBB damage aggregates and forms hotspots during epidemic conditions but is dispersed during endemic conditions (Hlásny et al. 2021). The formation of SBB damage hotspots has been previously identified in Poland (Stereńczak et al. 2020, Kamińska 2022) and is also common for other bark beetle species (Nelson and Boots 2008, Potter et al. 2016). We found that SBB damage was clearly aggregated into hotspots and recurrent hotspots in southeast Finland, despite a low global SA. Based on this, there are different levels of SA over large areas. However, dispersed hotspots also occurred in other parts of the study area. All these highlight the southeast region as a core area of SBB damage. The Etelä-Karjala Province had the highest proportion of recurrent hotspots (74.3%), corresponding to the high numbers of beetles reported in the annual pheromone monitoring of the species conducted by Natural Resources Institute Finland (Ylioja et al. 2023).

Hotspots presumably aggregated in areas with the most favourable conditions and resources for SBB, including a suitable climate, susceptible forests, and large beetle populations (Wermelinger 2004, Hlásny et al. 2021). The period with the highest number of hotspots (2012–14) was preceded by major windstorms in southeastern Finland, as well as a warm summer with higher temperature sums than the long-term average (Viiri et al. 2019, Tikkanen and Lehtonen 2023), resulting in large SBB damage (Pulgarín et al. 2024). The formation of a high number of hotspots could be attributed to this event, influenced by high numbers of suitable host trees and favourable environmental conditions for SBB reproduction. The outbreak likely subsided when weakened Norway spruces were cleared and thermal conditions and precipitation returned to a more normal level (Tikkanen and Lehtonen 2023).

The low recurrence of hotspots suggests that the conditions necessary for forming long-lasting clusters of damage were not consistently met. While spatial dependency in SBB damage is well documented—typically involving short-distance spread, <500 m (Kautz et al. 2011, Kärvemo et al. 2014b), and clustering during epidemic phases (Wermelinger 2004, Hlásny et al. 2021)—the concept of recurrent hotspots (i.e. locations that experience repeated damage over time) has not previously been explored for this species. In contrast, previous research has identified recurrent hotspots from *Drosophila ponderosa* lasting up to 2 years (Nelson and Boots 2008). However, to our knowledge, no previous research has shown comparable recurrence patterns for SBB. Our findings suggest that although spatial clustering does occur, it may not necessarily persist across years in the same locations, indicating a transient or dynamic spatial process.

The correlation between stand age and the hotspot formation suggests that older stands are more prone to becoming hotspots. This behaviour was similar to damage by *D. ponderosa*, which formed hotspots in the older stand age classes (Nelson and Boots 2008). According to our results, after salvage logging due to SBB damage, some of the remaining Norway spruce stands were of mature age, making them susceptible to SBB, as reported in previous research (Kärvemo et al. 2014a). Some previous research also suggests that age is not a key factor in determining new damage when attack densities are high over short distances, <500 m, such as in an epidemic phase and when hotspots are present (Mezei et al. 2014). These findings suggest that as Norway spruce stands grow and mature, they gradually reach a developmental stage more suitable for SBB hotspot formation. Mature trees generally offer larger diameters, thicker bark, and more phloem—conditions that favour beetle development over those in younger or slower-growing trees (Kärvemo et al. 2014a, Wermelinger 2004, Grunwald 1986). Still, our findings suggest that, in the long term, forest managers should avoid creating high-risk Norway spruce landscapes—those dominated by mature stands—in regions with high SBB risk (Hlásny et al. 2021).

The overall significant effect of stand development class on recurrent hotspots formation indicates that this variable influences the formation of recurrent hotspots collectively, even though none of the individual class contrasts were statistically significant. In an earlier study (Pulgarín et al. 2024), SBB showed a marked preference for mature stands and avoided other development classes, which may have influenced our results. Unlike Dmean and stand age, the effect of stand development class (or similar stand-level descriptors) on the formation of hotspots—or even SBB damage—has not been well investigated so far.

Based on our findings, the proximity to earlier SBB-damaged stands—that were salvage-logged—is the most influential variable for the formation of hotspots and recurrent hotspots. This is not surprising, as closely located SBB-damaged stands form hotspots and these hotspots might reoccur over time if damage continues in the surroundings. Importantly, the influence of SBB-damaged stands diminishes over time, with a weaker effect from SBB_{y-2} than from SBB_{y-1}. This suggests that SBB benefit more from resources generated by SBB damage in the prior year than from older damage, consistent with previous research (Gohli et al. 2024).

While we expected that earlier clear-cuts of any tree species would show a stronger association with hotspot formation and/or their recurrence, the association was more pronounced with prior SBB salvage logging operations, regardless of whether these involved clear-cuts or smaller-scale cuttings. The key seemed to be that hotspots were driven not just by clear-cuts but by areas that had prior SBB damage and were salvage logged as a result. Unfortunately, the dataset used did not contain information about the intensity or volume of the salvage logging. In previous research, an association between clear-cuts and new SBB damage has been observed in Sweden (Müller et al. 2022), Germany (Kautz et al. 2013), Central Europe (Grodzki et al. 2006), and Finland (Pulgarín et al. 2024). Clear-cuts create ideal conditions for beetle reproduction in the surrounding forest edges, as they commonly have wind-felled and weakened trees where the SBB population can grow (Kautz et al. 2013, Hroššo et al. 2020).

In our earlier study of the same study area by (Pulgarín et al. (2024), only a weak influence of SBB damage from previous years on new damage was found (also based on salvage logging data). In the present study, we found that proximity to prior-year damage is associated with the formation of hotspots and recurrent hotspots (Kärvemo et al. 2014a; Müller et al. 2022). This result is also related to SBB epidemics, when the beetles preferentially infect new hosts over short distances, regardless of host or site conditions, forming hotspots (Christiansen and Bakke 1988, Netherer et al. 2019). This has also been shown in *D. ponderosae* (Nelson and Boots 2008).

We assessed only a subset of the predisposing factors leading to the formation of SBB damage hotspots, focusing on forest and landscape variables. Other important factors, such as climate and beetle population dynamics (Wermelinger 2004, Hlásny et al. 2021, Kuhn et al. 2022), were not included. Previous research highlights temperature as a key climatic driver of SBB risk, particularly in northern Europe, where low temperatures limit beetle development and voltinism (Annila 1969, Battisti and Larsson 2015, Tikkanen and Lehtonen 2023). Additionally, drought weakens Norway spruce defences against insect pests, increasing vulnerability to damage (Netherer et al. 2015, Nardi et al. 2023). When high temperatures coincide with drought, rapidly growing beetle populations can cause severe attacks (Netherer et al. 2019). Future research should also use integrated climate variables and beetle population dynamics to better understand hotspot formation and its recurrence.

Conclusions

We found that SBB-damaged stands had a low global spatial autocorrelation but formed hotspots and recurrent hotspots at the local level. The formation of hotspots correlated with stand age and proximity to earlier SBB salvage logging operations. Whereas the formation of recurrent hotspots correlated with stand development class and proximity to earlier SBB salvage logging. As the distribution of SBB damage is not completely random, posterior analysis and correlation with other forest stand and landscape attributes require consideration of the distribution through space. The accurate and timely identification of core areas at risk of SBB damage, including hotspots and recurrent hotspots, requires active and precise identification of SBB damage. This is crucial for proper risk assessment and management activities. In addition to surveillance of visual symptoms from the ground, remote sensing could provide additional support for the detection of SBB-damaged stands. Such areas include areas with high occurrence of previous wind damage and/or SBB salvage logging and broad coverage of mature Norway spruce–dominated stands. In the long term, SBB damage risk should be considered in forest planning to improve resilience of managed forests to increasing climate-induced hazards.

To conclude, our findings on the drivers of SBB damage dispersion and hotspot formation provide support for evidence-informed risk management of SBB damage at the regional and national levels. However, further research is still needed to address the role of environmental factors (e.g. temperature and precipitation) on SBB damage, as well as on hotspot and recurrent hotspot formation.

Acknowledgements

Thanks to Suomen Metsäkeskus (Finish Forest Centre, www.metsakeskus.fi) for capturing, storing, curating, and making the information used in this study freely available. Special thanks to Juha Inkilä from Suomen Metsäkeskus for helping us to get familiar with the datasets. We are also grateful to the Finnish forest owners who supplied information to Suomen Metsäkeskus, making this research possible. The computational analyses in RStudio were performed on servers provided by the UEF Bioinformatics Center, University of Eastern Finland. The authors wish to acknowledge CSC – IT Center for Science, Finland, for computational resources for analysis. We also thank the editor Fabian Fassnacht and two anonymous reviewers for their constructive feedback and suggestions, which greatly improved the quality of the analysis and the manuscript.

Author contributions

John Alexander Pulgarín Díaz (Conceptualization of original idea, Data curation, Formal analysis, Investigation, Methodology, Software, Visualization, Writing—original draft, Writing—review & editing, Funding acquisition, Resources), Juliana Pérez-Pérez (Conceptualization of original idea, Formal analysis, Investigation, Methodology, Software, Validation, Visualization, Writing—original draft, Writing—review & editing), Markus Melin (Writing—review & editing. Heli Peltola: Funding acquisition, Project administration, Writing—review & editing), and Olli-Pekka Tikkanen (Project administration, Validation, Writing—review & editing)

Supplementary data

Supplementary data are available at *Forestry* online.

Conflict of interest

None declared.

Funding

This work was supported by the Research Council of Finland (former Academy of Finland) [grant numbers 357906, 359172 for

UNITE flagship]; European Union – NextGenerationEU instrument through the Research Council of Finland [grant number 353263 for Multirisk project]; LUMETO Doctoral programme in Science, Forestry and Technology at the University of Eastern Finland [to J.A.P.D.]; by EU funding under the Horizon Europe project Precilience [101157094 to M.M.]; and by Corporación Colombiana de Investigación Agropecuaria - AGROSAVIA [to J.A.P.D.].

Data availability

The datasets used are freely distributed by Metsäkeskus (www.metsakeskus.fi).

References

Annila E. Influence of temperature upon the development and voltinism of Ips Typographus L. (coleoptera, Scolytidae). *Ann Zool Fenn* 1969;**6**:161–208.

Anselin L. Local indicators of spatial association—LISA. *Geogr Anal* 1995;**27**:93–115.

Anselin L. The Moran scatterplot as an ESDA tool to assess local instability in spatial association. In: Fischer MM, (ed.). *Spatial Analytical Perspectives on GIS*. London: Routledge, 1996, 111–26.

Atkinson PM, Tate NJ. Spatial scale problems and geostatistical solutions: A review. *Prof Geogr* 2000;**52**:607–23.

Banerjee S, Carlin BP, Gelfand AE. *Hierarchical Modeling and Analysis for Spatial Data*. Boca Raton: CRC Press, 2015.

Battisti A, Larsson S. Climate change and insect Pest distribution range. In: Björkman C, Niemelä P, (eds.). *Climate Change and Insect Pests*. Wallingford: CABI, 2015, 1–15.

Bivand RS, Pebesma EJ, Gomez-Rubio V. *et al. Applied Spatial Data Analysis with R*. New York: Springer, 2008.

Bone C, Wulder MA, White JC. *et al.* A GIS-based risk rating of Forest insect outbreaks using aerial overview surveys and the local Moran's I statistic. *Appl Geogr* 2013;**40**:161–70.

Brooks ME, Kristensen K, van KJ. *et al.* GlmmTMB balances speed and flexibility among packages for zero-inflated generalized linear mixed modeling. *R J* 2017;**9**:378–400.

Brown JH, Mehlman DW, Stevens GC. Spatial variation in abundance. *Ecology* 1995;**76**:2028–43.

Brunsdon C, Comber L. *An Introduction to R for Spatial Analysis & Mapping*. London: Sage, 2015.

Christiansen E, Bakke A. The spruce bark beetle of Eurasia. In: Berryman AA, (ed.). *Dynamics of Forest Insect Populations: Patterns, Causes, Implications*, Boston: Springer, 1988, 479–503.

Darikwa TB, Manda SOM. Measuring bivariate spatial clustering in disease risks. In: Chen D-G, Manda S, Chirwa T, (eds.). *Modern Biostatistical Methods for Evidence-Based Global Health Research*, Cham: Springer, 2022, 235–60.

Diaz-Quijano FA. Regresiones Aplicadas al Estudio de Eventos Discretos En Epidemiología. *Salud UIS* 2016;**48**:9–15.

Dobor L, Hlásny T, Rammer W. *et al.* Is salvage logging effectively dampening bark beetle outbreaks and preserving Forest carbon stocks? *J Appl Ecol* 2019;**57**:67–76.

Eriksson M, Neuvonen S, Roininen H. Retention of wind-felled trees and the risk of consequential tree mortality by the European spruce bark beetle Ips Typographus in Finland. *Scand J For Res* 2007;**22**:516–23.

Finnish Meteorological Institute. *Ilmatieteenlaitos [Weather Institute (in Finnish)]*, 2022. https://www.ilmatieteenlaitos.fi/ilmastollinen-vertailukausi [accessed 18 February 2021].

Fox J, Weisberg S. *An R Companion to Applied Regression*. Thousand Oaks CA: SageThird, 2019.

Funke W, Petershagen M. Zur Flugaktivität von Borkenkäfern∗. *Jber Naturwiss Ver Wuppertal* 1994;**47**:5–10.

Getis A. Spatial autocorrelation. In: Fischer MM, Getis A, (eds.). *Handbook of Applied Spatial Analysis: Software Tools, Methods and Applications*. Berlin: Springer, 2010, 255–78.

Gohli J, Krokene P, Heggem ESF. *et al.* Climatic and management-related drivers of endemic European spruce bark beetle populations in boreal forests. *J Appl Ecol* 2024;**61**:809–20.

Gräler B, Pebesma E, Heuvelink G. Spatio-temporal interpolation using Gstat. *R J* 2016;**8**:204–18.

Grodzki W, Jakuš R, Lajzová E. *et al.* Effects of intensive versus No management strategies during an outbreak of the bark beetle Ips Typographus (L.) (Col.: Curculionidae, Scolytinae) in the Tatra mts. in Poland and Slovakia. *Ann For Sci* 2006;**63**:55–61.

Grunwald M. Ecological segregation of bark beetles (coleoptera, Scolytidae) of spruce. *J Appl Entomol* 1986;**101**:176–87.

Hardin JW, Hilbe JM. *Generalized Linear Models and Extensions*. Texas: Stata Press, 2007.

Hartig F. *DHARMa: Residual Diagnostics for Hierarchical (Multi-Level / Mixed) Regression Models*R Package Version 0.4.7. https://CRAN.R-project.org/package=DHARMa, 2024.

Hilbe JM. *Logistic Regression Models*. New York: CRC, 2009.

Hinze J, John R. Effects of heat on the dispersal performance of Ips Typographus. *J Appl Entomol* 2019;**144**:144–51. https://onlinelibrary.wiley.com/doi/abs/10.1111/jen.12718 [accessed 6 February 2021].

Hlásny T, König L, Krokene P. *et al.* Bark beetle outbreaks in Europe: State of knowledge and ways forward for management. *Curr For Rep* 2021;**7**:138–65.

Hof AR, Svahlin A. The potential effect of climate change on the geographical distribution of insect Pest species in the Swedish boreal Forest. *Scand J For Res* 2016;**31**:29–39.

Hroššo B, Mezei P, Potterf M. *et al.* Drivers of spruce bark beetle (Ips Typographus) infestations on downed trees after severe windthrow. *Forests* 2020;**11**:1290.

Kamińska A. Spatial autocorrelation based on remote sensing data in monitoring of Norway spruce dieback caused by the European spruce bark beetle Ips Typographus L. in the Białowieża Forest. *Sylwan* 2022;**11**:719–32.

Kärvemo S, Rogell B, Schroeder M. Dynamics of spruce bark beetle infestation spots: Importance of local population size and landscape characteristics after a storm disturbance. *For Ecol Manag* 2014b;**334**:232–40.

Kärvemo S, Van Boeckel TP, Gilbert M. *et al.* Large-scale risk mapping of an eruptive bark beetle–importance of Forest susceptibility and beetle pressure. *For Ecol Manag* 2014a;**318**:158–66.

Kautz M, Schopf R, Ohser J. The "sun-effect": Microclimatic alterations predispose Forest edges to bark beetle infestations. *Eur J For Res* 2013;**132**:453–65.

Kautz M, Dworschak K, Gruppe A. *et al.* Quantifying Spatio-temporal dispersion of bark beetle infestations in epidemic and non-epidemic conditions. *For Ecol Manag* 2011;**262**:598–608.

Korhonen KT, Ahola A, Heikkinen J. *et al.* Forests of Finland 2014–2018 and their development 1921–2018. *Silva Fenn* 2021;**55**:49.

Kuhn A, Hautier L, Martin GS. Do pheromone traps help to reduce new attacks of Ips Typographus at the local scale after a sanitary cut? *PeerJ* 2022;**10**:e14093. https://peerj.com/articles/14093 [accessed 12 March 2025].

Lausch A, Heurich M, Fahse L. Spatio-temporal infestation patterns of Ips Typographus (L.) in the Bavarian Forest National Park, Germany. *Ecol Indic* 2013;**31**:73–81.

Lindman L, Ranius T, Schroeder M. Regional climate affects habitat preferences and thermal sums required for development of the

Eurasian spruce bark beetle, Ips Typographus. *For Ecol Manag* 2023;**544**:121216.
Louis M, Dohet L, Grégoire J. Fallen trees' last stand against bark beetles. *For Ecol Manag* 2015;**359**:44–50.
Lüdecke D. Ggeffects: Tidy data frames of marginal effects from regression models. *J Open Source Softw* 2018;**3**:772.
Mehtätalo L, Lappi J. *Biometry for Forestry and Environmental Data: With Examples in R*. Boca Raton: CRC, 2020.
Metsäkeskus. *Metsävarakuviot [Description about the Forest Stand Database (in Finnish)]*, 2021. Available at https://www.metsakeskus.fi/sites/default/files/document/tietotuotekuvaus-metsavarakuviot.pdf.
Metsäkeskus. *Metsävaratiedon Laatu [Quality of Forest Resource Information (in Finnish)]*, 2025. https://www.metsakeskus.fi/fi/avoin-metsa-ja-luontotieto/tietojen-yllapito/tiedon-laatu [accessed 5 March 2025].
Mezei P, Grodzki W, Blaženec M. *et al.* Host and site factors affecting tree mortality caused by the spruce bark beetle (Ips Typographus) in mountainous conditions. *For Ecol Manag* 2014;**331**:196–207.
Morales M, López L. Estudio de Homogeneidad de La Dispersión En Diseño a una Vía de Clasificación Para Datos de Proporciones y Conteos. *Rev Colomb Estad* 2009;**32**:59–78.
Morales M, Lozano J. Prueba de Homogeneidad de La Dispersión Para Datos de Proporción Sobredispersos Mediante Regresión Beta. *Integr Temas Mat* 2014;**32**:55–70.
Moran P. Notes on continuous stochastic phenomena. *Biometrika* 1950;**37**:17–23.
Müller M, Olsson P, Eklundh L. *et al.* Features predisposing Forest to bark beetle outbreaks and their dynamics during drought. *For Ecol Manag* 2022;**523**:120480.
Nardi D, Jactel H, Pagot E. *et al.* Drought and stand susceptibility to attacks by the European spruce bark beetle: A remote sensing approach. *Agric For Entomol* 2023;**25**:119–29.
Nelson TA, Boots B. Detecting spatial hot spots in landscape ecology. *Ecography* 2008;**31**:556–66.
Netherer S, Matthews B, Katzensteiner K. *et al.* Do water-limiting conditions predispose Norway spruce to bark beetle attack? *New Phytol* 2015;**3**:1128–41.
Netherer S, Panassiti B, Pennerstorfer J. *et al.* Acute drought is an important driver of bark beetle infestation in Austrian Norway spruce stands. *Front For Glob Change* 2019;**2**:21.
Nygren M. The basic setting for growing trees. In: Rantala S, (ed.). *Finnish Forestry. Practice and Management*. Keuruu: Metsäkustannus Oy, 2011, 1–34.
O'Sullivan D, Unwin DJ. *Geographic Information Analysis*. New Jersey: John Wiley & Sons, 2010.
Økland B, Nikolov C, Krokene P. *et al.* Transition from windfall-to patch-driven outbreak dynamics of the spruce bark beetle Ips Typographus. *For Ecol Manag* 2016;**363**:63–73.
Pebesma E. Simple features for R: Standardized support for spatial vector data. *R J* 2018;**10**:439–46.
Pebesma E, Bivand R. *Spatial Data Science: With Applications in R. Boca Raton*: Taylor & Francis, 2023.
Perez-Perez J, Diaz P, Alexander J. *et al.* Effect of socioeconomic strata and land cover on dengue hotspots in Medellin, Colombia. *Am J Trop Med Hyg* 2025;**112**:1–11.
Pinheiro JC, Bates D. *Mixed-Effects Models in S and S-PLUS, Mixed-Effects Models in S and S-PLUS*. New York: Springer, 2000.
Potter KM, Koch FH, Oswalt CM. *et al.* Data, data everywhere: Detecting spatial patterns in fine-scale ecological information collected across a continent. *Landsc Ecol* 2016;**31**:67–84.
Pulgarín JA, Melin M, Ylioja T. *et al.* Relationship between stand and landscape attributes and Ips Typographus salvage loggings in Finland. *Silva Fenn* 2024;**58**:23069.
Rhodes JR, McAlpine CA, Zuur AF. *et al.* GLMM applied on the spatial distribution of koalas in a fragmented landscape. In: Zuur AF, Ieno EN, Walker NJ. et al., (eds.). *Mixed Effects Models and Extensions in Ecology with R*. New York: Springer, 2009, 469–92.
RStudio Team. *RStudio: Integrated Development Environment for R*. Boston: RStudio, 2023.
Salas D, Sánchez DY, Achury G. *et al.* Malaria En Poblaciones con Ocupación Minera, Colombia, 2012-2018. *Biomedica* 2021;**41**:121–30. https://doi.org/10.7705/biomedica.5899.
Sexton JP, McIntyre PJ, Angert AL. *et al.* Evolution and ecology of species range limits. *Annu Rev Ecol Evol Syst* 2009;**40**:415–36.
Siabato W, Guzmán-Manrique J. La Autocorrelación Espacial y El Desarrollo de La Geografía Cuantitativa. *Cuad Geogr Rev Colomb Geogr* 2019;**28**:1–22.
Sikkink PG, Zuur AF, Ieno EN. *et al.* Monitoring for change: Using generalised least squares, non-metric multidimensional scaling, and the mantel test on western Montana grasslands. In: Zuur A, Leno E, Smith GM, (eds.). *Analysing Ecological Data*. New York: Springer, 2007, 463–84.
Siljander M, Uusitalo R, Pellikka P. *et al.* Spatiotemporal clustering patterns and sociodemographic determinants of COVID-19 (SARS-CoV-2) infections in Helsinki, Finland. *Spat Spatio-Temporal Epidemiol* 2022;**41**:100493.
Stereńczak K, Mielcarek M, Modzelewska A. *et al.* Intra-annual Ips Typographus outbreak monitoring using a multi-temporal GIS analysis based on hyperspectral and ALS data in the Białowieża forests. *For Ecol Manag* 2019;**442**:105–16.
Stereńczak K, Mielcarek M, Kamińska A. *et al.* Influence of selected habitat and stand factors on bark beetle Ips Typographus (L.) outbreak in the Białowieża Forest. *For Ecol Manag* 2020;**459**:117826.
Tikkanen OP, Lehtonen I. Changing climatic drivers of European spruce bark beetle outbreaks: A comparison of locations around the northern Baltic Sea. *Silva Fenn* 2023;**57**:23003.
Tobin PC, Haynes KJ, Carroll AL. Spatial dynamics of Forest insects. In: Allison JD, Paine TD, Slippers B. *et al.*, (eds.). *Forest Entomology and Pathology: Volume 1: Entomology*, Vol. **i**. Switzerland: Springer, 2023, 647–68. https://link.springer.com/chapter/10.1007/978-3-031-11553-0_18.
Venäläinen A, Lehtonen I, Laapas M. *et al.* Climate change induces multiple risks to boreal forests and forestry in Finland: A literature review. *Glob Chang Biol* 2020;**26**:4178–96. https://doi.org/10.1111/gcb.15183.
Viiri H, Viitanen J, Mutanen A. *et al.* Metsätuhot Vaikuttavat Euroopan Puumarkkinoihin – Suomessa Vaikutukset Toistaiseksi Vähäisiä [Forest damage affects the European timber market – in Finland the effects are minor so far (in Finnish)]. *Metsätieteen Aikakauskirja* 2019;**2019**:7.
Washaya P, Modlinger R, Tyšer D. *et al.* Patterns and impacts of an unprecedented outbreak of bark beetles in Central Europe: A glimpse into the future? *For Ecosyst* 2024;**11**:100243.
Wermelinger B. Ecology and Management of the Spruce Bark Beetle Ips Typographus— A review of recent research. *For Ecol Manag* 2004;**202**:67–82.
Wermelinger B, Seifert M. Temperature-dependent reproduction of the spruce bark beetle Ips Typographus, and analysis of the potential population growth. *Ecol Entomol* 1999;**24**:103–10. https://onlinelibrary.wiley.com/doi/full/10.1046/j.1365-2311.1999.00175.x [accessed 10 March 2022].

Ylioja T, Kokkonen J, Aarnio L. *et al.* Kirjanpainajan Esiintymisen Seuranta [spruce bark beetle monitoring]. In: Terhonen E, Melin M, (eds.). *Metsätuhot Vuonna 2022 [Forest Damage in the Year 2022] Luonnonvara- Ja Biotalouden Tutkimus* 48/2023. Helsinki: Luonnonvarakeskus, 2023, 56–68.

Zuur AF, Ieno EN, Walker NJ. *et al.* Required pre-knowledge: A linear regression and additive modelling example. In: Zuur AF, Ieno EN, Walker NJ. et al., (eds.). *Mixed Effects Models and Extensions in Ecology with R*. New York: Springer, 2009, 531–52.

Forestry: An International Journal of Forest Research, 2025, 1–14
https://doi.org/10.1093/forestry/cpaf058
Original Article